Evaluation of Segmental Interaction by Small-Angle X-ray Scattering Based on the Random-Phase Approximation for Asymmetric, Polydisperse Triblock Copolymers

Shinichi Sakurai,† Keiji Mori,‡ Atsuo Okawara,§ Kohtaro Kimishima, and Takeji Hashimoto*

Department of Polymer Chemistry, Faculty of Engineering, Kyoto University, Kyoto 606, Japan

Received October 17, 1991; Revised Manuscript Received January 20, 1992

ABSTRACT: The binary segmental interaction parameter, χ_{S-B}, for poly(styrene-*block*-butadiene-*block*-styrene) (SBS) triblock copolymer was evaluated by analyzing the small-angle X-ray scattering (SAXS) in the disordered state based on the random-phase approximation (RPA) for asymmetric and polydisperse triblock copolymers. The parameter fitting allowed us to determine also the radius of gyration, R_g, of an entire copolymer from the peak position of the scattered intensity. Samples used in this study are Shell's TR-1102 and Kraton D-1102 having the weight fractions of polystyrene 0.31 and 0.28, respectively. The effects of asymmetry in the size of the repeating units and polydispersity in molecular weight on the scattering function and on the evaluation of χ and R_g for these particular SBS's were examined. The analyses gave the temperature (T) dependence of χ_{S-B} as $\chi_{S-B} = 6.59 \times 10^{-3} + 13.6/T$ and the statistical segment length of polybutadiene, b_{PB}, calculated from the value of R_g, as $b_{PB} = 0.65 \pm 0.02$ nm, for both TR-1102 and D-1102. The theory with no polydispersity or no asymmetry correction turned out to overestimate χ_{S-B} and the R_g values for these block copolymers.

I. Introduction

Block copolymer is a unique polymeric material which possibly exhibits highly ordered patterns of the structure with an identity period of a few tens of nanometers and size of "grain" in a few microns. It is worth studying their morphologies from the viewpoint of pattern formation in condensed matter. Recently it has been found that there is a possibility of controlling the morphology in various fashions through modifying the architecture of the polymer. It is also interesting to study the morphological transition of the patterns having the highly ordered structure.

The microphase-separation transition (MST) or the order–disorder transition[1-21] (ODT) of block copolymers is also an interesting phenomenon well-known from the earlier stage of work and has been studied intensively by means of various methods, e.g., by small-angle X-ray scattering (SAXS),[1-8] small-angle neutron scattering (SANS),[9-13] and dynamic mechanical measurements.[6,14,15] The scattering experiments[1-13,23-26] revealed a dominant mode of the concentration fluctuation with a wavenumber q equal to q_m ($\sim 1/R_g$ where R_g is the radius of gyration of the entire block copolymer) existing in the disordered state, which was theoretically explained as *the correlation hole effect*.[9] SAXS from the block copolymer melts and solutions in the disordered state has been studied theoretically.[9,16-31] Leibler[16] has calculated the structure factor for a diblock copolymer in bulk and the disordered state in the context of Landau-type *mean-field* theory using the random-phase approximation (RPA) method, as a function of f and a product χN, where f is the volume fraction of one of the block chains, χ the Flory interaction parameter per segment, and N the degree of polymerization (DP) for an entire block copolymer. In addition, the RPA and other theories permit calculations of structure factors for various molecular architectures.[17,18,23,27,30] Thus, it is a great advantage to use the scattering theory in order to evaluate χ for the various types of copolymers.

Recently, Landau-type *mean-field* theory has been generalized to take into account the Brazovskii effect,[32] and what is called the finite size effect[19-22] has been explored. The theory was extended to solutions.[20,21,25] This effect may cause a considerable effect in the evaluation of χ. Some authors have taken this effect into account.[11,26] On the other hand, the effects of polydispersity and composition distribution[13,22,24,27,29] and those of asymmetry in segment size[31] are also important and have been considered in the calculation of the structure factor of the diblock copolymer in the disordered state.

For the evaluation of χ values for poly(styrene-*block*-butadiene-*block*-styrene) (SBS) triblock copolymer we developed the RPA theory for a triblock copolymer which takes into account correction for polydispersities in molecular weight and composition as well as that for asymmetry in segment size. The parameter fitting between the theoretical and experimental SAXS profiles allowed us to determine χ values and also the statistical segment length. The content of this paper is as follows. First, we discuss the effects of polydispersity and asymmetry on the evaluation of χ and R_g. Second, we compare χ values thus obtained and their temperature dependencies of the segmental interaction between styrene and butadiene with the literature values. Owens et al.[7] have evaluated χ values as a function of temperature from the scattering function obtained in the disordered state for a poly(styrene-*block*-butadiene) (SB) diblock copolymer by synchrotron SAXS. They used the scattering theory for polydisperse block copolymers along with the physical parameters corrected for the asymmetry in the segment size. However, the theory itself did not explicitly include the asymmetry correction. Hewel et al.[8] have also obtained the χ values as a function of T. They measured the SAXS profiles from SB diblock copolymers in the bulk state as a function of temperature using synchrotron SAXS. Then they determined the spinodal temperature, T_s, for ODT of a

† Present address: Department of Polymer Science and Engineering, Kyoto Institute of Technology, Matsugasaki, Kyoto 606, Japan.
‡ Present address: Research Center, Toyobo Co., Ltd., Katata, Ohtsu, Shiga 520-02, Japan.
§ Present address: Research Center, Asahi Glass Co., Ltd., Yokohama 221, Japan.

0024-9297/92/2225-2679$03.00/0

given polymer by extrapolating the inverse scattered intensity at the scattering maximum in the disordered state, I_{max}^{-1}, to zero in a plot of I_{max}^{-1} vs T^{-1}. The spinodal χ value, χ_s, for the given polymer was evaluated using Leibler's theory[16] which gives a $(\chi N)_s$ value for a given block copolymer composition. Consequently, the relationship between χ_s and T_s in the form of $\chi_s = A + B/T_s$ has been obtained. In the original Leibler's theory, however, it should be noted that the effects of polydispersities in molecular weight and composition and the asymmetry in the segment size are not taken into account.

II. Theoretical Background

In the previous work,[31] the effects of polydispersities in molecular weight and composition and the asymmetry in the segment size on the scattering function have been investigated for a diblock copolymer and have been found to be significant in some cases. Using a similar procedure, we develop the *mean-field* theory for the asymmetric and polydisperse triblock copolymers to express the scattering function, $I(q)$, in the disordered state where q is the magnitude of the scattering vector defined by

$$q = (4\pi/\lambda) \sin(\theta/2) \tag{1}$$

with λ and θ being the wavelength of X-rays and the scattering angle, respectively.

The system treated here is a A1–B–A2 type triblock copolymer with DP's being N_{A1}, N_B, and N_{A2}, respectively. Note that the A1 and A2 block chains comprise the same monomers A but have different DP's. A total DP of the triblock copolymer, N_C, is given by $N_C = N_{A1} + N_B + N_{A2}$. Taking the asymmetry in the segment size into account, we define the effective DP for Kth component, r_K, as

$$r_K = (v_K/v_0)N_K \quad (K = \text{A1, B, or A2}) \tag{2}$$

where v_A ($=v_{A1} = v_{A2}$) and v_B denote the molar volumes of segment A and B, respectively, and v_0 denotes the molar volume of the reference cell. v_K is given by $M_{u,K}/\rho_K$, where $M_{u,K}$ is the molecular weight of the Kth segment, and ρ_K is the density of the K polymer. We assume here $v_0 = (v_A v_B)^{1/2}$. For an entire block copolymer the total effective DP, r_C, is given by $r_C = r_{A1} + r_B + r_{A2}$. Then the effective fraction, f_K, is defined by

$$f_K = r_K/r_C = v_K N_K/(v_A N_{A1} + v_B N_B + v_A N_{A2}) \tag{3}$$

and $f_{A1} + f_B + f_{A2} = 1$.

The SAXS intensity is expressed as:

$$I(q) = \boldsymbol{K}(a-b)^2\left[\frac{\overline{S(q)}}{\overline{W(q)}} - 2\chi\right]^{-1} \tag{4}$$

with

$$\overline{S(q)} = \langle S_{AA}(q)\rangle_\nu + 2\langle S_{AB}(q)\rangle_\nu + \langle S_{BB}(q)\rangle_\nu \tag{5}$$

and

$$\overline{W(q)} = \langle S_{AA}(q)\rangle_\nu\langle S_{BB}(q)\rangle_\nu - \langle S_{AB}(q)\rangle_\nu^2 \tag{6}$$

where the line over the quantity indicates that it contains volume-averaged quantities. $\boldsymbol{K}$ is a proportional constant. $\langle ... \rangle_\nu$ designates the volume average in terms of Schultz–Zimm's distribution function for molecular weights. a and b denote the electron densities of the A and B monomers, respectively. The correlation functions $S_{AA}(q)$, $S_{BB}(q)$, and $S_{AB}(q)$ in eqs 5 and 6 can be calculated as follows. For the asymmetric triblock copolymer

$$S_{AA}(q) = \left(\frac{v_A}{v_0}\right)^2 \frac{1}{r_C}\sum_{i,j=1}^{N_C}\delta_i\delta_j P_{ij}(q) \tag{7}$$

$$S_{BB}(q) = \left(\frac{v_B}{v_0}\right)^2 \frac{1}{r_C}\sum_{i,j=1}^{N_C}(1-\delta_i)(1-\delta_j)P_{ij}(q) \tag{8}$$

$$S_{AB}(q) = \left(\frac{v_A}{v_0}\right)\left(\frac{v_B}{v_0}\right)\frac{1}{r_C}\sum_{i,j=1}^{N_C}\delta_i(1-\delta_j)P_{ij}(q) \tag{9}$$

with

$$P_{ij}(q) = \exp[-\langle R^2\rangle_{ij}q^2] \tag{10}$$

where δ_i denotes the δ function which is defined to be unity only when the A segment is placed on the ith position in the polymer chain. The same goes for δ_j when the A segment is placed on the jth position. $\langle R^2\rangle_{ij}$ denotes a mean-squared distance between the ith and jth positions. Using the $P_{ij}(q)$ function for a Gaussian chain, the results are expressed by

$$S_{AA}(q) = r_C\{f_{A1}^2 g_{A1}^{(2)}(q) + 2f_{A1}f_{A2}g_{A1}^{(1)}(q)\, g_{A2}^{(1)}(q)\exp(-x_B) + f_{A2}^2 g_{A2}^{(2)}(q)\} \tag{11}$$

$$S_{BB}(q) = r_C f_B^2 g_B^{(2)}(q) \tag{12}$$

$$S_{AB}(q) = r_C\{f_{A1}g_{A1}^{(1)}(q) + f_{A2}g_{A2}^{(1)}(q)\}f_B g_B^{(1)}(q) \tag{13}$$

with

$$g_K^{(1)}(q) = \frac{1}{x_K}[1 - \exp(-x_K)] \tag{14}$$

and

$$g_K^{(2)}(q) = \frac{2}{x_K^2}[x_K - 1 + \exp(-x_K)] \tag{15}$$

where

$$x_K = N_K b_K^2 q^2/6 \tag{16}$$

and b_K is the statistical segment length of the Kth segment (K = A1, B, or A2). Equation 15 is the Debye function. Note that eqs 11–13 are reduced to the correlation functions for a symmetric triblock copolymer[23,27] when $b_A = b_B$ and $v_A = v_B$. Let us show the result for an A–B–A type triblock copolymer, which is the special case of an A1–B–A2 type with $N_{A1} = N_{A2}$.

$$S_{AA}(q) = 2r_C f_A^2\{g_A^{(2)}(q) + [g_A^{(1)}(q)]^2\exp(-x_B)\} \tag{17}$$

$$S_{BB}(q) = r_C f_B^2 g_B^{(2)}(q) \tag{18}$$

$$S_{AB}(q) = 2r_C f_A f_B g_A^{(1)}(q)\, g_B^{(1)}(q) \tag{19}$$

The volume-averaged quantities in eqs 5 and 6 are calculated as

$$\begin{pmatrix}\langle S_{AA}(q)\rangle_\nu \\ \langle S_{BB}(q)\rangle_\nu \\ \langle S_{AB}(q)\rangle_\nu\end{pmatrix} = \int_0^\infty\int_0^\infty\int_0^\infty dN_{A1}\, dN_B\, dN_{A2}\, \phi(N_{A1},N_B,N_{A2})\begin{pmatrix}S_{AA}(q) \\ S_{BB}(q) \\ S_{AB}(q)\end{pmatrix} \tag{20}$$

where $\phi(N_{A1},N_B,N_{A2})$ is the normalized volume distribu-

tion function of the copolymers having the DP's N_{A1}, N_B, and N_{A2} for A1, B, and A2 block chains, respectively. $\phi(N_{A1},N_B,N_{A2})$ is given by

$$\phi(N_{A1},N_B,N_{A2}) = \frac{\varphi(N_{A1},N_B,N_{A2})\{(N_{A1}+N_{A2})v_A + N_B v_B\}}{\int_0^\infty\int_0^\infty\int_0^\infty dN_{A1}\,dN_B\,dN_{A2}\,\varphi(N_{A1},N_B,N_{A2})\{(N_{A1}+N_{A2})v_A + N_B v_B\}} \quad (21)$$

using the number distribution function of the copolymers $\varphi(N_{A1},N_B,N_{A2})$. We assume that the number distributions of the molecular weights for A1, B, and A2 block chains are independent of each other and given by Schultz-Zimm's distribution function. Then

$$\varphi(N_{A1},N_B,N_{A2}) = \varphi_{A1}(N_{A1})\,\varphi_B(N_B)\,\varphi_{A2}(N_{A2}) \quad (22)$$

with

$$\varphi_K(N_K) = \frac{\nu_K^{k_K+1}N_K^{k_K}}{\Gamma(k_K+1)}\exp(-\nu_K N_K) \quad (23)$$

$$\nu_K = \frac{k_K+1}{N_{K,n}} = \frac{k_K+2}{N_{K,w}} \quad (24)$$

or

$$\frac{N_{K,w}}{N_{K,n}} = \frac{k_K+2}{k_K+1} \equiv \lambda_K \quad (25)$$

where $N_{K,n}$ and $N_{K,w}$ are the number- and weight-average DP (K = A1, B, or A2). Note that $\varphi_K(N_K)$ given by eqs 23 and 24 is the normalized number distribution. In this case the denominator in the right-hand side of eq 21 is given by

$$\int_0^\infty\int_0^\infty\int_0^\infty dN_{A1}\,dN_B\,dN_{A2}\,\varphi(N_{A1},N_B,N_{A2})\times\{(N_{A1}+N_{A2})v_A + N_B v_B\} = v_A\left(\int_0^\infty \varphi_{A1}(N_{A1})\,N_{A1}\,dN_{A1} + \int_0^\infty \varphi_{A2}(N_{A2})\,N_{A2}\,dN_{A2}\right) + v_B\int_0^\infty \varphi_B(N_B)\,N_B\,dN_B = (N_{A1,n}+N_{A2,n})v_A + N_{B,n}v_B = r_{C,n}v_0$$

And then $\phi(N_{A1},N_B,N_{A2})$ is given by

$$\phi(N_{A1},N_B,N_{A2}) = \varphi_{A1}(N_{A1})\,\varphi_B(N_B)\,\varphi_{A2}(N_{A2})\,r_C/r_{C,n} \quad (26)$$

The heterogeneity index of the molecular weight, $M_{K,w}/M_{K,n}$, for each block chain has the following relationship with M_w/M_n for the entire triblock copolymer, i.e.

$$\frac{M_w}{M_n} - 1 = \left(\frac{M_{A1,w}}{M_{A1,n}} - 1\right)w_{A1}^2 + \left(\frac{M_{B,w}}{M_{B,n}} - 1\right)w_B^2 + \left(\frac{M_{A2,w}}{M_{A2,n}} - 1\right)w_{A2}^2 \quad (27)$$

where w_K denotes the weight fraction defined by

$$w_K = \frac{M_{K,n}}{M_{A1,n}+M_{B,n}+M_{A2,n}} \quad (28)$$

and $M_{K,n}$ and $M_{K,w}$ are the number- and weight-average molecular weights for K block chains, respectively, and M_n and M_w are the number- and weight-average molecular weights for the entire triblock chain, respectively. For the case of the A–B–A type triblock copolymer, the following relation should be used.

$$\frac{M_w}{M_n} - 1 = 2\left(\frac{M_{A,w}}{M_{A,n}} - 1\right)w_A^2 + \left(\frac{M_{B,w}}{M_{B,n}} - 1\right)w_B^2 \quad (29)$$

Hence, $\lambda_K = N_{K,w}/N_{K,n} = M_{K,w}/M_{K,n}$ needed in the calculation of eq 20 via k_K can be evaluated from the data on M_w/M_n if we assume that $\lambda_{A1} = \lambda_B = \lambda_{A2}$. The analytical results of integrations of eq 20 are given in Appendix A (see eqs A.1–A.15).

It should be noted that for symmetric block copolymers the volume-averaged quantities in eqs 5 and 6 are equal to the weight-averaged quantities. In this case the averaged quantities can be obtained by replacing $\phi(N_{A1},N_B,N_{A2})$ in eq 20 with $\Psi(N_{A1},N_B,N_{A2})$, the normalized weight distribution function of the copolymers having DP's N_{A1}, N_B, and N_{A2} for A1, B, and A2 block chains, respectively. In our previous analysis,[24] we assumed that the weight distributions of the molecular weights for A and B block chains of an A–B diblock copolymer are independent, i.e.

$$\Psi(N_A,N_B) = \Psi_A(N_A)\,\Psi_B(N_B) \quad (30)$$

instead of assuming the number distributions independent, as described by eq 22 for the triblock copolymer. Here $\Psi_K(N_K)$ is equal to the right-hand side of eq 23 with

$$\nu_K = \frac{k_K}{N_{K,n}} = \frac{k_K+1}{N_{K,w}} \quad (31)$$

or

$$\frac{N_{K,w}}{N_{K,n}} = \frac{k_K+1}{k_K} \equiv \lambda_K \quad (32)$$

Note that $\Psi_K(N_K)$ given with eq 31 or eq 32 is the normalized weight distribution; i.e.

$$\int_0^\infty N_K\Psi_K(N_K)\,dN_K = N_{K,w}$$

If the quantities $\langle S_{KJ}(q)\rangle_\nu$ are calculated using eqs 30 and 31, the final expressions become very complex as shown in ref 24 for diblock copolymers and in Appendix C for A–B–A triblock copolymers (see eqs C.1–C.16). However, in terms of reaction kinetics, it seems more reasonable to assume independence of the number distributions rather than that of the weight distributions for respective block chains. Consequently, we recommend a present approach of calculating $\langle S_{KJ}(q)\rangle_\nu$ with eq 26 rather than our previous approach[24] with eq 30. In Appendix B we show the quantities $\langle S_{KJ}(q)\rangle_\nu$ calculated for asymmetric, polydisperse diblock copolymers based upon the present approach (see eqs B.1–B.3).

The scattering theory for the melt was extended to the semidilute solution of the block copolymers in the disordered state.[20,21,28] It was shown that the scattering function $I(q)$ is enormously simplified in the context of the pseudo-binary approximation[3,25,33]

$$I(q) = \boldsymbol{K}(a-b)^2\phi_P\left[\frac{\overline{S(q,R_g)}}{\overline{W(q,R_g)}} - 2\chi_{eff}\right]^{-1} \quad (33)$$

in which χ, R_g, and $(a-b)^2$ in the melts are replaced by χ_{eff}, R_g, and $(a-b)_{eff}^2 \equiv (a-b)^2\phi_p$ in the presence of the solvent. This pseudo-binary approximation was shown to be valid under the optical Θ condition and for the nonselective solvent.[25] Furthermore, a renormalization group analysis[33] showed that χ_{eff} is given in the semidilute Θ solution by

$$\chi_{eff} = \frac{\chi\phi_p^2}{\phi_p + \chi/u_{12}^*} \quad (34)$$

where u_{12}^* is the fixed point to be nearly equal to 10 (see eq 3.12 of ref 33). It should be noted that χ_{eff} in eq 34 corresponds to $\chi_{eff}\phi_p$ in eq 3.25b of ref 33. In the weak-to-moderate segregation limit satisfying

$$\chi/u_{12}^* \ll \phi_p \quad (35)$$

χ_{eff} becomes identical to that expected in the limit of the

Table I
Sample Characteristics

sample	M_n (osmometry)	M_w/M_n (GPC)	w_{PS}	ρ, g/cm^3	microstructure of PB (^{13}C NMR) 1,2	cis-1,4	trans-1,4
TR-1102	5.9×10^4	1.2 ± 0.15^a	0.31[b]		7.4	55.6	37.0
Kraton D-1102	5.7×10^4	1.2 ± 0.15^a	0.28[c]	0.94[c]	9.8	36.6	53.6

[a] The value of M_w/M_n obtained by GPC varies within 0.15 depending on the apparatus used. [b] Calculated from ^{13}C NMR data (19 mol % styrene segment). [c] Catalogue values.

dilution approximation, i.e.

$$\chi_{eff} = \phi_p \chi \tag{36}$$

In fact for our experimental condition, $\phi_p = 0.71$ and $\chi/u_{12}^* \cong 3.6 \times 10^{-3}$ for D-1102 (see section III for the specimen codes and section IV for the χ values). Thus eq 35 is satisfied and the dilution approximation of eq 36 is valid. Moreover, it is experimentally confirmed directly, as will be discussed later in section IV in conjunction with Figure 5, that the concentration covered in our experiments satisfied the semidilute Θ condition so that the block copolymers are locally swollen but globally unperturbed; i.e., the radius of gyration R_g in the solution is that for the unperturbed chain. The semidilute Θ condition is also confirmed theoretically because f_0 in eq 3.1b of ref 33 (which is on the order of 0.01) is much smaller than ϕ_p. Therefore, the experimental SAXS profiles will be analyzed in section IV using eqs 33 and 36 where $S(q)/W(q)$ is given by eqs 5 and 6 and by eqs A.13–A.15 given in Appendix A.

III. Experimental Section

The samples used are supplied by Shell Co., Ltd. Table I shows results of the sample characterizations, where M_n and the heterogeneity index of molecular weight, M_w/M_n, are obtained by the membrane osmometry and by GPC, respectively. The data of the weight fraction of PS, w_{PS}, are picked up from Shell's commercial catalogue. The polybutadiene block of TR-1102 and that of D-1102 were characterized to have microstructures of 7% 1,2-linkage, 56% cis-1,4-linkage, and 37% trans-1,4-linkage and 10% 1,2-linkage, 37% cis-1,4-linkage, and 53% trans-1,4-linkage, respectively, by ^{13}C NMR.

The common solvent dioctyl phthalate (DOP) was used to reduce the binary segmental interaction between styrene and butadiene so as to lower the order–disorder transition temperature, T_{ODT}, of the block copolymer solution in the range from room temperature to a degradation temperature of the polymer. The concentrated or semidilute polymer solutions of 60 and 67 wt % TR-1102 and 70, 80, 90, and 100 wt % D-1102 with DOP were prepared via solvent casting with methylene chloride. A mixture of the polymer and DOP was dissolved in an excess amount of methylene chloride to obtain a homogeneous solution of a ca. 5 wt % mixture of the polymer and DOP, and then methylene chloride was gradually evaporated in an oven kept at ca. 30 °C. Methylene chloride is a common solvent for the mixtures and has a low boiling temperature of ca. 40 °C. Complete removal of methylene chloride was ensured by measuring the weight of the solution periodically until a constant weight was attained. The volume fractions of polymer, ϕ_p, studied are 0.61 and 0.68 for TR-1102 and 0.71, 0.81, 0.90, and 1.00 for D-1102.

SAXS measurements were performed with an apparatus[34] consisting of a 12-kW rotating-anode X-ray generator, a graphite crystal for the incident beam monochromatization, a 1.5-m camera, and a one-dimensional position-sensitive proportional counter (PSPC). Cu Kα radiation with a wavelength of λ = 0.154 nm was used. The SAXS profiles were corrected for an absorption due to the specimen, an air scattering, and the thermal diffuse scattering arising from the density fluctuations. Since the incident beam with a line-shaped cross section was irradiated to the unoriented specimens, the scattering profiles were further desmeared.[35] The absolute scattered intensity for D-1102/DOP-(ϕ_p=0.71) was obtained by the nickel-foil method.[36] The SAXS profiles were measured in situ at each temperature where the samples were first preheated for 5 min to ensure thermal equilibration and then subjected to measurements for 30 min in order to get sufficient statistical accuracy. To avoid the thermal degradation of the specimens as much as possible, new samples were used for the measurements of D-1102 with ϕ_p of 0.90 and 1.00 at each temperature higher than 240 °C.

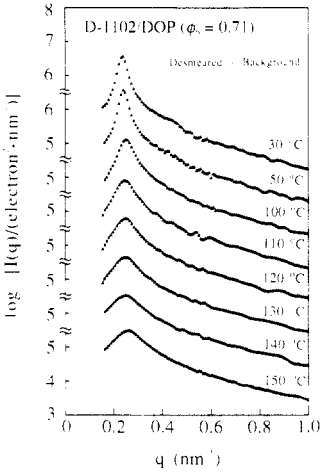

Figure 1. Semilogarithmic plots of scattered intensity $I(q)$ vs q at various temperatures for D-1102/DOP(ϕ_p=0.71).

IV. Results and Discussion

A. ODT and Determination of Mean-Field ODT.

SAXS profiles of $I(q)$ vs q observed at various temperatures are shown in a semilogarithmic plot for D-1102/DOP-(ϕ_p=0.71) in Figure 1. These profiles were measured in situ at the designated temperatures by cooling the specimens stepwise from the highest measuring temperature, 150 °C. SAXS profiles exhibit at least one scattering maximum. The scattering vector q_m for the first-order maximum yields the wavelength D ($\equiv 2\pi/q_m$) of the dominant mode of the concentration fluctuations. In the disordered state this wavelength D corresponds to the wavelength D_{dis} for the dominant mode of the fluctuations which are activated by thermal energy, whereas in the ordered state it corresponds to the spacing for the domain structure generated by the segregation power. For evaluation of the χ value, the SAXS profile obtained in the disordered state should be analyzed. Therefore, it is necessary to determine T_{ODT} first.

In the disordered state, one single scattering maximum should be observed due to the *correlation hole effect*,[9] as experimentally confirmed by many investigators.[1-13,23-26] Actually one can see that all the scattering profiles observed above 50 °C show the single scattering maximum. However, it is not correct to take these profiles as those in the disordered state because higher order scattering maxima due to microdomain structures become very weak in the vicinity of the ODT. Therefore, T_{ODT} should be determined quantitatively on the basis of the following criteria, if one wishes to follow the criterion of the Landau-type *mean-field* approximation.[16] In the disordered state, (i) the position q_m of the scattering maximum or D_{dis} is

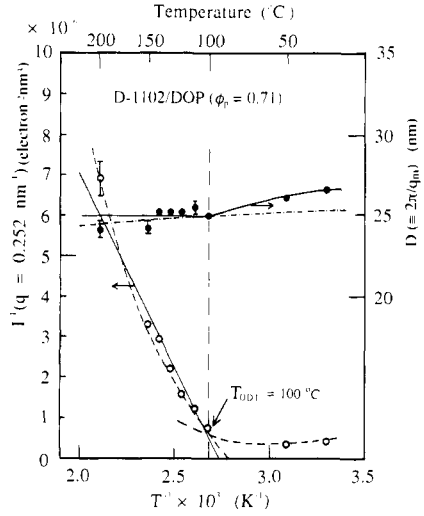

Figure 2. Inverse of the scattered intensity at $q = 0.252$ nm^{-1}, $I^{-1}(q=0.252\ \text{nm}^{-1})$, and D ($=2\pi/q_m$), where q_m is the q-value at the first-order scattering maximum, plotted against the inverse of the absolute temperature, T^{-1}, for D-1102/DOP(ϕ_p=0.71).

independent of T except for the minor temperature dependence attributed to the temperature changes of the radius of gyration, R_g of the polymer coil, and (ii) the inverse of the scattered intensity at any given q satisfying $qR_g \lesssim 1$ linearly decreases with increasing χ. If the temperature change of χ is given by $\chi = A + B/T$ as found in most of the experimental results, then $I^{-1}(q)$ at a given q linearly decreases with increasing T^{-1} (for $B > 0$). Therefore

$$D_{dis} \sim T^0 \tag{37}$$

$$I^{-1}(q) \sim (\text{constant} - \chi) \sim (1 - \text{constant} \times T^{-1}) \tag{38}$$

or

$$I^{-1}(q_m) \sim \left(\frac{1}{T_s} - \frac{1}{T}\right) \tag{39}$$

where T_s is the *mean-field* spinodal temperature. The deviations from eqs 37 and 38 or eq 39 are expected to be observed by further increasing T^{-1} as a result of the onset of the ordering and microdomain formation.

Let us present here a determination of ODT in the context of the Landau-type mean-field approximation as described above. Figure 2 shows the *mean-field* analysis on the ODT as described above in which $I^{-1}(q)$ at $q = q_m = 0.252\ \text{nm}^{-1}$, the wavenumber for the scattering maximum in the profile at 100 °C, and D are plotted against T^{-1}. In this approximate method, deviations from the relations expressed by eqs 37 and 38 or eq 39 reflect the *mean-field* ODT. The data on D and I^{-1} obtained at $T \geq T_{ODT} = 100 \pm 5$ °C can be approximated by eqs 37 and 39 as shown by the corresponding straight (solid) lines in this figure. Both D and I^{-1} start to deviate from the straight lines at $T = T_{ODT}$. Therefore, the mean-field T_{ODT} is evaluated to be 100 ± 5 °C. The *mean-field* T_s was estimated to be 91 ± 4 °C by extrapolating the linear relationship between $I^{-1}(q_m)$ and T^{-1} to $I^{-1}(q_m) = 0$ so as to find the intercept with the abscissa.

The figure also includes the temperature change of a quantity f(T) by a dash-and-dot line. f(T) is defined by

$$f(T) = D(T=T^\circ)\left[\frac{\langle R^2(T)\rangle_0}{\langle R^2(T=T^\circ)\rangle_0}\right]^{1/2} = D(T=T^\circ)\exp[(T-T^\circ)\kappa/2] \tag{40}$$

where $\langle R^2(T)\rangle_0$ is the mean-square end-to-end distance of the unperturbed block copolymer chains at a given T, T° is a reference temperature, and κ is the temperature coefficient of the unperturbed chain dimensions of the block copolymer defined as $\kappa \equiv \text{d ln } \langle R^2(T)\rangle_0/\text{d}T$. The dash-and-dot line is the temperature variation of f(T) given by eq 40 with $T^\circ = 100$ °C and $\kappa = -0.3 \times 10^{-3}$ [K^{-1}] for this particular case.[37] The quantity f(T) represents the temperature variation of the spacing $D(T)$ if it arises only from the thermal expansivity of the unperturbed chain dimension. The temperature variation of $D(T)$ can be nicely followed by f(T) for $T \geq 100$ °C ($=T_{ODT}$) but is much larger than f(T) for $T < 100$ °C. The large discrepancy at $T < 100$ °C indicates that the increase of the spacing D with lowering T is due to the chain extension as a consequence of the microphase separation rather than due to the thermal expansion of the chain.

At a first glance, the data of I^{-1} as a function of T^{-1} appear to be curved over the entire temperature range covered. However, a close observation of the curve would reveal that the variation of I^{-1} vs T^{-1} at $T \geq T_{ODT}$ is distinctly different from that at $T < T_{ODT}$. It appears to be reasonable to break the entire curve into the two separate curves as drawn by the two dashed curves, i.e., one at $T > T_{ODT}$ and the other at $T < T_{ODT}$. The curve at $T < T_{ODT}$ does not exist along the curve extrapolated from the curve at $T \geq T_{ODT}$ but is rather bent upward against the extrapolated curve. Moreover, as a matter of fact, I^{-1} tends to increase with lowering T or increasing T^{-1}. Note that the data on I^{-1} are at a fixed q (=0.252 nm^{-1}) at which the scattered intensity was approximately maximum at $T \geq T_{ODT}$. The increase of I^{-1} or the intensity drop as the temperature is lowered in the ordered state clearly reflects a sharpening of the scattering peak around $q = 0.252\ \text{nm}^{-1}$ and a shift of a scattering maximum toward a lower q, both of which clearly manifest the onset of the microphase separation, i.e., an ordering phenomenon of block copolymers in the ordered state. This upward bend of I^{-1} vs T^{-1} in the ordered state is therefore parallel to the upward deviation of D vs T^{-1} from the dash-and-dot line corresponding to f(T). It should be noted that the deviation of the dashed curve at $T < T_{ODT}$ from the straight line on I^{-1} vs T^{-1} at $T \geq T_{ODT}$ is much greater than the deviation of the dashed curve at $T \geq T_{ODT}$ from the straight line.

It should be worthy to comment here about deviations from the Landau-type *mean-field* behavior on the ODT of our systems. Two types of deviations have been pointed out either theoretically[19] or experimentally:[11,12] (1) the finite size effect (Brazovskii effect), which makes the ODT weakly first-order,[11,19] and (ii) the chain stretching,[12] which was proposed to occur in the disordered state slightly above the ODT.

The finite size effect was found to induce concave curvature in the plot of $I^{-1}(q)$ vs T^{-1}. This effect may be discernible also in our plots even at $T \gtrsim T_{ODT}$ shown in Figure 2 (compare the corresponding dashed curve and the straight line). However, in our case the deviation from the linearity between $I^{-1}(q)$ and T^{-1} which starts to develop at $T \lesssim T_{ODT}$ is much stronger than the deviation which is manifested as the weak concave curvature in the disordered state. This makes the finite size effect in our system less remarkable than that in the system studied by Bates et al.[11,12]

The chain stretching in the disordered state near the ODT was claimed to be observed by measuring D or q_m at a fixed T as a function of N (degree of polymerization, DP) through the ODT. In our experiments in which N is fixed but T is varied, the corresponding chain stretching

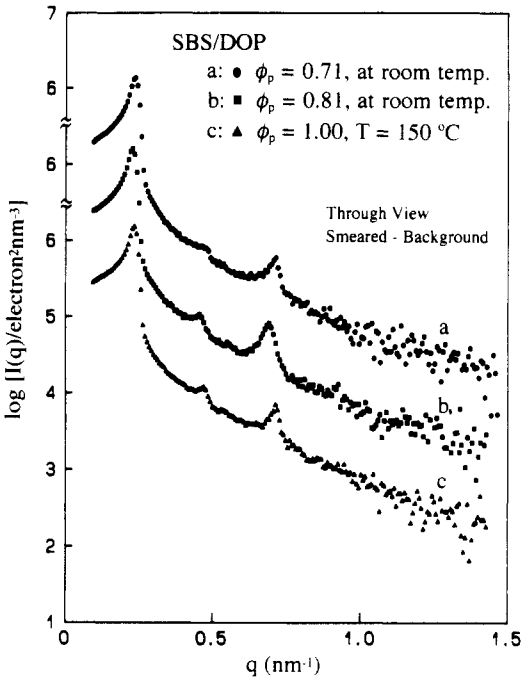

Figure 3. Plots of log $I(q)$ vs q at various temperatures for the DOP solutions of the SBS specimen having $M_n = 6.31 \times 10^4$, $M_w/M_n = 1.15$, and $w_{PS} = 0.56$. These were obtained by irradiating X-rays to the film specimens from the direction perpendicular to the film surface (through view). Profiles a–c are for $\phi_p = 0.71$ at room temperature (●), $\phi_p = 0.81$ at room temperature (■), and $\phi_p = 1.00$ at 150 °C (▲), respectively.

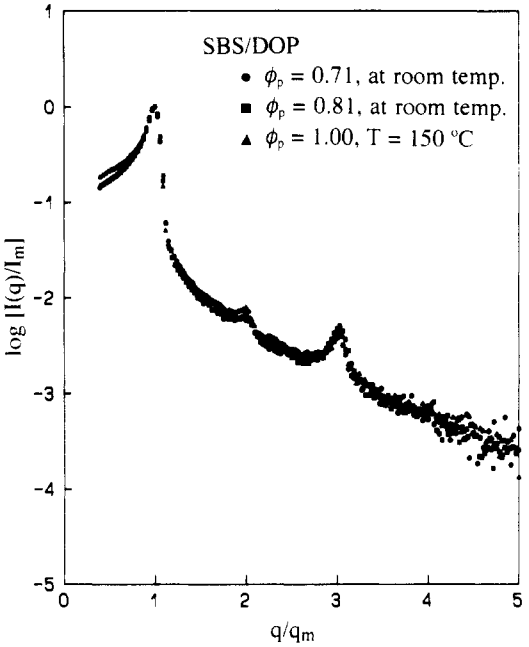

Figure 4. Plots of log $[I(q)/I_m]$ vs q/q_m for the same three samples shown in Figure 3, i.e., for the SBS/DOP with $\phi_p = 0.71$ at room temperature (●), $\phi_p = 0.81$ at room temperature (■), and $\phi_p = 1.00$ at 150 °C (▲). I_m and q_m denote the intensity and the q value of the first-order scattering maximum, respectively.

may be possibly observed in the temperature dependence of D_{dis}, because the change of N at a fixed T or χ corresponds to the change of T or χ at a fixed N (note that χN is the relevant parameter). This chain stretching in the disordered state may cause an increase of D_{dis} with increasing χ or decreasing T toward the ODT. However, it is important to note that the degree of chain stretching, if any, may not change strongly by changing T because χ only weakly depends on T. As will be shown later, χ_{ODT}

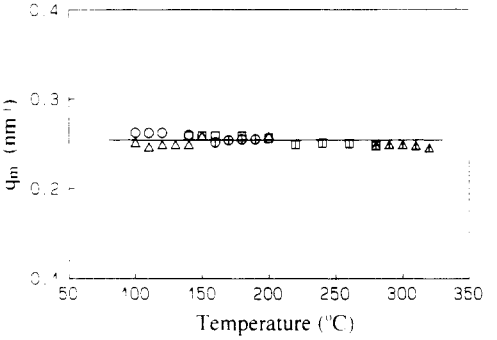

Figure 5. Plot of q_m as a function of temperature for TR-1102/DOP(ϕ_p=0.61 (○) and 0.68 (□)) and D-1102/DOP(ϕ_p=0.71 (△), 0.81 (◐), 0.90 (▣), and 1.00 (▲)).

$- \chi_u)/\chi_{ODT} = 0.09$ for D-1102/DOP(ϕ_p=0.71), where χ_{ODT} and χ_u are the χ parameters at the ODT and the highest temperature covered in our experiments, respectively. These values are much less than the value $(N_{ODT} - N_{GST})/N_{ODT} = 0.43$ reported by Bates et al.[12] where N_{ODT} and N_{GST} are respectively the N value at which the ODT occurs and that at which the transition from a Gaussian coil to a stretched coil occurs in the disordered state. Thus, in our systems the weak chain stretching in the disordered state, if there is, is considered to be essentially independent of T over the temperature range covered in our experiments. The increase of D below the ODT reflects a strong chain stretching accompanied by the domain formation induced by increasing segregation power.[2,3,5]

B. Neutrality of DOP. Since the dilution approximation of eq 36 is used to determine χ from χ_{eff} values, the solvent DOP should be a neutral and Θ solvent for both PS and PB block chains. At first, we show that DOP is a neutral solvent. For this purpose we used the other SBS triblock copolymer which forms a lamellar microdomain structure. M_n, M_w/M_n, and w_{PS} of this specimen are 6.31×10^4, 1.15, and 0.56, respectively, as analyzed by osmometry, GPC, and elementary analysis. The microstructure of PB block chains of this specimen are 33, 55, and 12 mol % for cis-1,4-, trans-1,4-, and 1,2-linkages, respectively, which are almost identical to those of Kraton D-1102. In Figure 3 the SAXS profiles of the DOP solutions of this SBS specimen are shown. These were obtained by irradiating X-rays to the film specimens from the direction perpendicular to the film surface (through view). Profiles a–c are for $\phi_p = 0.71$ at room temperature, $\phi_p = 0.81$ at room temperature, and $\phi_p = 1.00$ at 150 °C, respectively. Since all the profiles exhibit three scattering maxima of which a relative ratio of q values can be assigned as an integer, the lamellar microdomains turned to be formed in these samples. If the solvent DOP is a neutral solvent, DOP swells both PS and PB lamellae by the same extent, and hence the volume ratio of PS and PB lamellae is expected to be conserved upon adding DOP. However, the domain spacing changes with a change of the effective repulsive interaction between PS and PB block chains, which depends on ϕ_p and T. In addition, the scattered intensities depend on the effective contrast between PS- and PB-rich phases and the number of lamellae existing in the irradiated volume of the sample. Therefore, in order to check the conservation of the volume ratio of PS and PB lamellae for those three samples with different ϕ_p and T, the SAXS profiles should be scaled, using reduced scattered intensities and reduced q. Semilogarithmic plots of $I(q)/I_m$ vs q/q_m for the three samples are shown in Figure 4 where I_m and q_m denote the intensity and the q value of the first-order scattering maximum, respectively. One can see that the three profiles overlap onto the same master

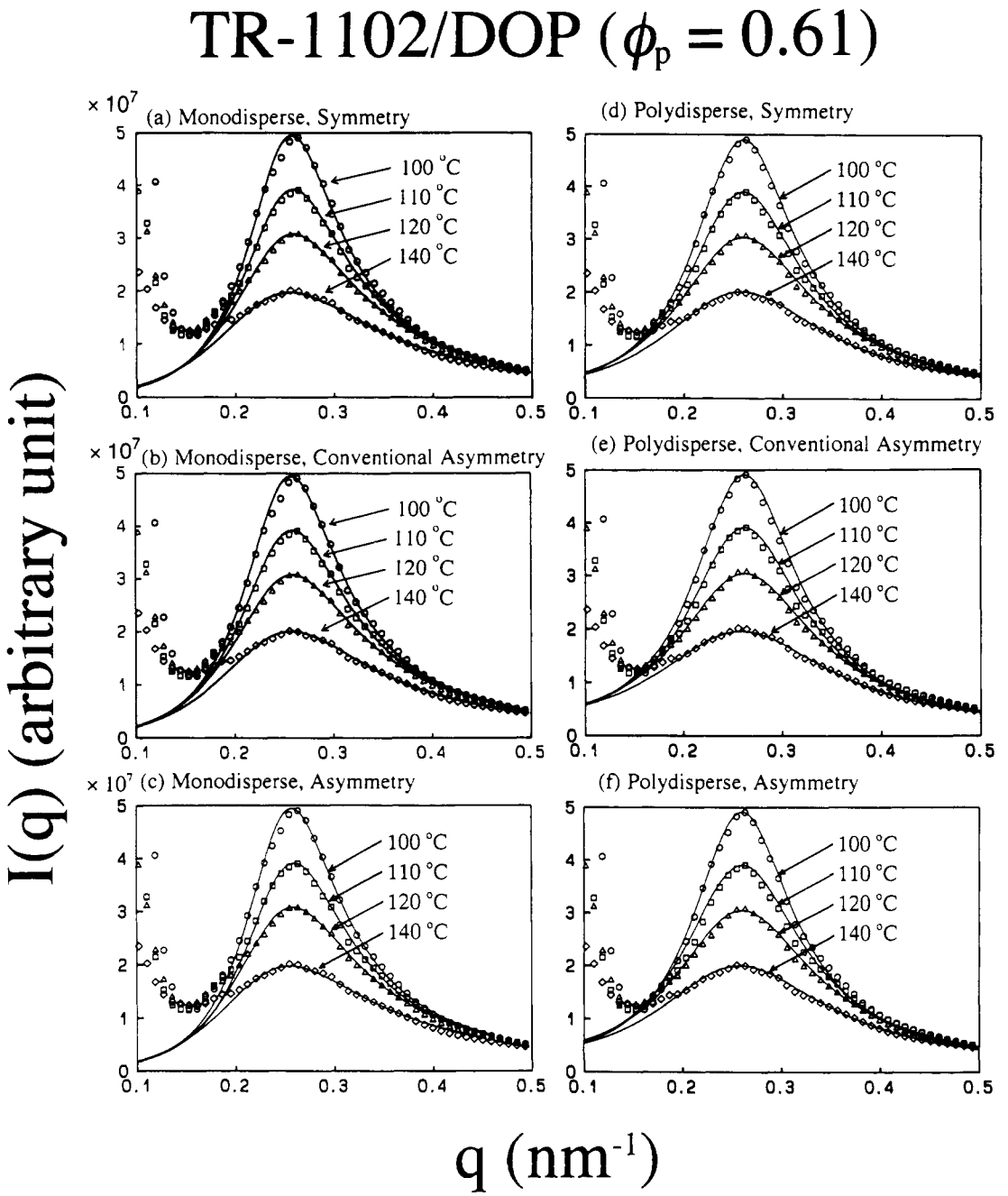

Figure 6. Best fits between the experimental and theoretical scattering profiles shown in plots of $I(q)$ vs q for TR-1102/DOP(ϕ_p=0.61) at 100 (○), 110 (□), 120 (△), and 140 °C (◇). The solid curves are the calculated scattering profiles using the RPA without polydispersity and asymmetry corrections (a), without polydispersity but with conventional asymmetry corrections (b), without polydispersity but with asymmetry corrections (c), with polydispersity but without asymmetry corrections (d), with polydispersity and conventional asymmetry corrections (e), and with polydispersity and asymmetry corrections (f).

curve. This clearly suggests that the volume fraction does not change by adding DOP and hence that DOP is a neutral solvent for the SBS triblock copolymer.

C. Confirmation of the Semidilute Θ Condition. We now show experimental evidence that the DOP solutions studied here form semidilute Θ solutions for the polystyrene–polybutadiene block copolymer so that their q_m's for the scattering profile in the disordered state or R_g's are independent of ϕ_p. Figure 5 is a plot of q_m as a function of temperature for various polymer concentrations. As discussed later, the R_g values of TR-1102 and D-1102 calculated from the literature value of the segment lengths are almost identical so that the q_m values for the two specimens can be compared directly. It is clearly seen that the q_m value and hence R_g are independent of polymer concentration ϕ_p ($0.6 \lesssim \phi_p \leq 1.0$) and temperature T ($100 \leq T \leq 320$ °C) covered in this experiment, within experimental error. This suggests that the SBS/DOP solutions studied in this work are semidilute Θ solutions.

D. Polydispersity and Asymmetry Effects and Determination of χ, R_g, and b_{PB}. Let us next discuss the effect of polydispersity and asymmetry in the segment size on the scattering function and on the evaluation of χ and R_g for these particular SBS's. For this purpose parameter fittings between the experimental and theoretical scattering profiles were performed using χ, R_g, and $K(a - b)^2$ as floating parameters for TR-1102/DOP-(ϕ_p=0.61).[38] We do not recommend comparison of the experimental and theoretical profiles in the absolute intensity. This is simply because (i) a small error in the calibration constant K causes a significant error in the derived value of χ, (ii) a small error in the estimation of the scattering constant, i.e., $(a - b)^2$, causes a significant error in the derived value of χ (the estimation of $(a - b)^2$

Table II
Results Obtained for TR-1102/DOP(ϕ_p=0.61) by the Best Fits between the Experimental and Theoretical SAXS Profiles by the Various Methods,[a] As Shown in Figure 6

	R_g, nm					
T, °C	a	b	c	d	e	f
100	11.06	10.45	10.98	8.91	7.71	8.10
110	11.01	10.40	10.88	8.91	7.71	8.10
120	11.01	10.40	10.93	8.91	7.71	8.10
140	11.16	10.45	11.09	9.00	7.82	8.20
	b_{PB},[b] nm					
T, °C	a	b	c	d	e	f
100	0.930	0.871	0.923	0.722	0.601	0.641
110	0.925	0.867	0.913	0.722	0.601	0.641
120	0.925	0.867	0.918	0.722	0.601	0.641
140	0.940	0.871	0.933	0.731	0.612	0.651

[a] Methods a–f employed here correspond to those used for calculations of the theoretical scattering profiles in parts a–f of Figure 6, respectively: without polydispersity and asymmetry corrections (a), without polydispersity but with conventional asymmetry corrections (b), without polydispersity but with asymmetry corrections (c), with polydispersity but without asymmetry corrections (d), with polydispersity and conventional asymmetry corrections (e), or with polydispersity and asymmetry corrections (f). [b] The statistical segment length of PB, b_{PB}, is calculated from the R_g value using eq 41 with b_{PS} = 0.70 nm.[39]

requires mass densities of A and B block chains in the disordered state which are not necessarily well characterized), and (iii) $\boldsymbol{K}(a-b)^2$ affects only the absolute intensity level but does not affect the shape of the scattering curve. (Hence, $\boldsymbol{K}(a-b)^2$ is independent of the determination of χ and the statistical segment lengths which affect the shape of the scattering curve.)

In the calculations of the scattering function, the following parameters are used: $b_A = b_{PS}$ = 0.70 nm,[39] ρ_{PS} = 0.970 g/cm^3 for $T > T_g$,[40] ρ_{BP} = 0.928 g/cm^3. This value of ρ_{PB} is evaluated from the data of D-1102, i.e., ρ = 0.94 g/cm^3 (density of D-1102) and w_{PS} = 0.28 (see Table I). Figure 6 shows best fits where the theoretical scattering functions are shown by solid lines. The theoretical scattering functions shown in parts a and b of Figure 6 were obtained for the case of no polydispersity correction and no asymmetry correction, those in part c of Figure 6 for the case of no polydispersity correction but asymmetry correction, those in parts d and e of Figure 6 for the case of polydispersity correction but no asymmetry correction, and those in part f of Figure 6 for the case of polydispersity correction and asymmetry correction. In parts b and e of Figure 6, however, $f_{K,n} = v_K N_{K,n}/(2v_A N_{A,n} + v_B N_{B,n})$ was used in the calculations instead of $f_{K,n} = N_{K,n}/(2N_{A,n} + N_{B,n})$. We designate hereafter this method as a *conventional asymmetry correction*.

Without polydispersity correction, the fitting between experimental and theoretical scattering functions is poor in the angular region smaller than q_m, especially in $0.15 \le q \le 0.20$ nm^{-1} (see Figure 6a–c). Contrary to this, with polydispersity correction the theoretical scattering functions were better fitted to data in the region of $0.15 \le q \le 0.5$ nm^{-1} (see Figure 6d–f). Consequently, the polydispersities in molecular weight and composition turned out to increase the scattered intensities in the angular region smaller than q_m. Compared to the effect of the correction on the fitting precision of the profiles, the effect on the derived values of χ and the statistical segment length is much larger, as will be shown in Table II and Figure 7. The obvious upturn of $I(q)$ in $q < 0.15$ nm^{-1} may be attributed to the scattering arising from the concentration fluctuation of the SBS polymer as a whole in the solution,

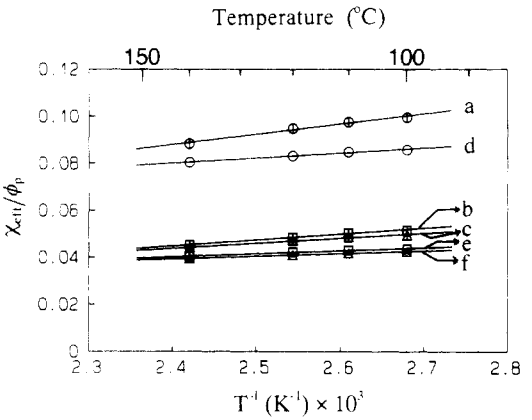

Figure 7. Binary segmental interaction parameter, χ_{S-B}, which is given as χ_{eff}/ϕ_p, plotted against the inverse of absolute temperature, T^{-1}, for TR-1102/DOP(ϕ_p=0.61). The χ_{eff} values were evaluated by the best fits between the experimental and theoretical SAXS profiles by the various methods, as shown in Figure 6. Methods a–f employed here correspond to those used for calculations of the theoretical scattering profiles in parts a–f of Figure 6, respectively.

which has the scattering maximum at q = 0, or to the artifacts caused by foreign particles.

The effects of asymmetry in the segment size on the scattering profile and of the fitting precision are found to be trivial, less than the effects of polydispersity, although the asymmetry significantly affects the absolute value of χ determined by the fitting, as the polydispersity does.

Figure 7 is a plot of χ_{eff}/ϕ_p vs the inverse of the absolute temperature where χ_{eff} denotes the χ value obtained by the fitting. χ_{eff}/ϕ_p is identical to the segmental interaction parameter between styrene and butadiene, χ_{S-B}, in the bulk state, since eq 36 is applicable to our system, i.e., the semidilute Θ solution with the weak-to-moderate interaction limit of $\chi/u_{12}^* < \phi_p$.[25,33] The obtained R_g values for an entire copolymer and the values of the statistical segment length of polybutadiene, b_{PB}, are summarized in Table II. The b_{PB} values were calculated from the R_g values together with the data on the degrees of polymerization of the respective block chains and the literature value of the segment length for PS[39] (b_{PS} = 0.70 nm) using the following relationship between R_g of the entire block copolymer and $R_{g,K}$ of the K block chain:

$$R_g^2 = 2R_{g,A}^2 + R_{g,B}^2 = (2N_{A,n}b_A^2 + N_{B,n}b_B^2)/6 \quad (41)$$

Irrespective of the methods used for the fitting, the temperature dependence of the segmental interaction parameter can be expressed as $\chi_{eff}/\phi_p = \chi_{S-B} = A + B/T$. When the polydispersity correction is made, the χ_{S-B} value and the R_g value evaluated by the fitting are considerably smaller compared to those evaluated by the theory with no correction (cf. lines a and d, b and e, or c and f in Figure 7 and the values in a and d, b and e, or c and f columns of Table II). In the case when the theory with the asymmetry correction is used, the evaluated χ value is smaller than that obtained by the theory without the asymmetry correction (cf. lines a and c or d and f in Figure 7). As for the conventional asymmetry correction, the evaluated χ_{S-B} values are comparable to the values estimated from the theory with the asymmetry correction (cf. lines b and c or e and f in Figure 7). This indicates that the conventional asymmetry correction in the composition of block copolymer can be a good approximation for the polystyrene–polybutadiene block copolymer system, even if the theory itself does not include explicitly the asymmetry correction. The values b_{PB} evaluated by

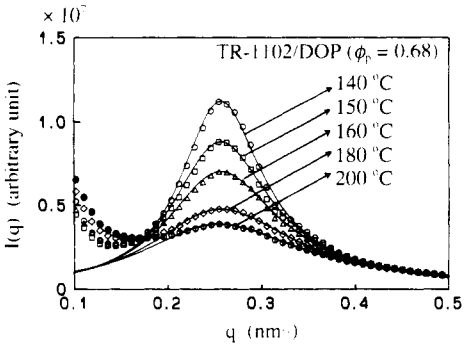

Figure 8. Best fits between the experimental and theoretical scattering profiles for TR-1102/DOP(ϕ_p=0.68) at 140 (○), 150 (□), 160 (△), 180 (◇), and 200 °C (⊕). The solid curves are the calculated scattering profiles.

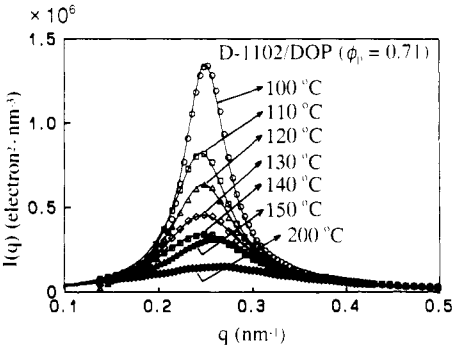

Figure 9. Best fits between the experimental and theoretical scattering profiles for D-1102/DOP(ϕ_p=0.71) at 100 (○), 110 (□), 120 (△), 130 (◇), 140 (▥), 150 (▲), and 200 °C (◈).

method f are consistent with the literature value, i.e., b_{PB} = 0.65 nm for PB with 7% 1,2-linkage, 36% cis-1,4-linkage, and 57% trans-1,4-linkage (from the viscosity measurement)[41] and b_{PB} = 0.69 nm for PB with 20% 1,2-linkage, 36% cis-1,4-linkage, and 44% trans-1,4-linkage (from the small-angle neutron scattering measurement).[42] This means that the theory with no polydispersity or no asymmetry correction overestimates the R_g value for the polystyrene–polybutadiene block copolymer system. We then used method f (the theory involving both the polydispersity and the asymmetry corrections) hereafter to evaluate χ and R_g values for the other specimens.

The best fits between the experimental and theoretical SAXS profiles for TR-1102/DOP(ϕ_p=0.68) and D-1102/DOP(ϕ_p=0.71)[38] are shown in Figures 8 and 9, respectively. The theoretical profiles involve both the polydispersity and the asymmetry corrections. Figure 8 for TR-1102/DOP(ϕ_p=0.68) covers the SAXS profiles at higher temperatures, compared to the profiles shown in Figure 6. The R_g value is independent of temperature and polymer concentration, as discussed above, and is 8.15 ± 0.28 nm for both TR-1102 and D-1102, which gives b_{PB} = 0.65 ± 0.02 nm, again consistent with the literature values. Let us next discuss the interaction parameter χ_{S-B} obtained by using the theory with the two kinds of corrections. The χ_{eff} values at each temperature are tabulated in Table III for TR-1102/DOP(ϕ_p=0.61 and 0.68) and D-1102/DOP-(ϕ_p=0.71, 0.81, 0.90, and 1.00). The χ_{S-B} values given by χ_{eff}/ϕ_p are plotted as a function of the inverse of the absolute temperature, T^{-1}, in Figure 10. It is found that χ_{S-B} obtained from the TR-1102 and D-1102 solutions are identical, having the same temperature dependence, i.e., the data points fall on the same straight line over the temperature range covered in our experiments. In the previous paper,[43] the value χ_{S-B} is strongly affected by the

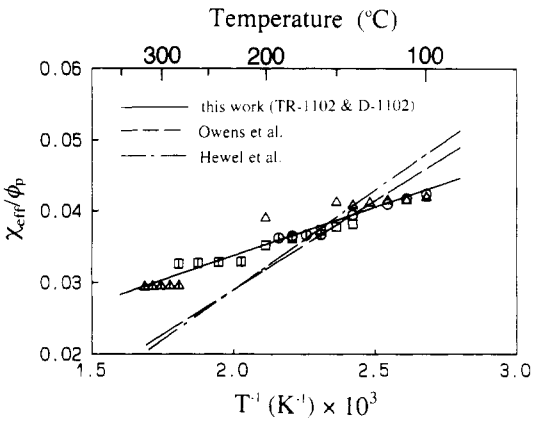

Figure 10. Binary segmental interaction parameter, χ_{S-B}, which is given as χ_{eff}/ϕ_p, plotted against the inverse of the absolute temperature, T^{-1}, for TR-1102/DOP(ϕ_p=0.61 (○) and 0.68 (□)) and D-1102/DOP(ϕ_p=0.71 (△), 0.81 (⊕), 0.90 (▥), and 1.00 (▲)). The literature values on χ_{S-B} are shown together in the figure: Owens et al.[7] (– –) and Hewel et al.[8] (– · –).

Table III
χ_{eff} Values at Each Temperature for TR-1102/DOP(ϕ_p=0.61 and 0.68) and D-1102/DOP(ϕ_p=0.71, 0.81, 0.90 and 1.00)

	TR-1102/DOP		D-1102/DOP			
T, °C	ϕ_p = 0.61	ϕ_p = 0.68	ϕ_p = 0.71	ϕ_p = 0.81	ϕ_p = 0.90	ϕ_p = 1.00
100	0.0258		0.0299			
110	0.0254		0.0296			
120	0.0249		0.0296			
130			0.0293			
140	0.0240	0.0260	0.0291			
150		0.0257	0.0294			
160		0.0254		0.0297		
170				0.0297		
180		0.0246		0.0296		
190				0.0293		
200		0.0239	0.0278			
220					0.0298	
240					0.0297	
260					0.0296	
280					0.0295	0.0298
290						0.0297
300						0.0297
310						0.0296
320						0.0296

microstructure of PB, especially the content of the 1,2-linkage. Since the microstructures of PB for TR-1102 and D-1102 are not identical, the temperature dependence of χ_{S-B} should be separately examined for each SBS. However, we obtained the temperature dependence of χ_{S-B} ($\equiv\chi_{eff}/\phi_p$) as given by

$$\chi_{S-B} = 6.59 \times 10^{-3} + 13.6/T \quad (42)$$

for the two samples. This may be because the contents of the 1,2-linkage are, respectively, 7 and 10% for TR-1102 and D-1102, which are considered to be the same within experimental error of measuring microstructures by ^{13}C NMR.

The temperature dependencies of χ_{S-B} from the literature are also shown in Figure 10 to facilitate comparison. These are

$$\chi_{S-B} = -0.021 + 25/T \quad (43)$$

obtained by Owens et al.[7] for an SB diblock copolymer in bulk with $M_n = 1.86 \times 10^4$ (by osmometry), M_w/M_n = 1.06 (by GPC), w_{PS} = 0.49 (by ultraviolet measurement), and

95% 1,2-linkage of PB and

$$\chi_{S\text{-}B} = -0.027 + 28/T \quad (44)$$

by Hewel et al.[8] for SB diblock copolymers in bulk with $f = 0.3$ and $1.80 \times 10^4 \leq M \leq 4.00 \times 10^4$ (the definition of fraction f and molecular weight M and the microstructure of PB were not specified in their paper). Owens et al. have evaluated the $\chi_{S\text{-}B}$ values by analyzing the SAXS profiles with the theory corrected for polydispersity but not for asymmetry. However, they used physical parameters corrected for asymmetry so that their method is similar to our conventional asymmetry correction. On the other hand, Hewel et al. have determined χ_s values as a function of T_s in the form of $\chi_s = A + B/T_s$ by synchrotron SAXS through changing the molecular weight of SB diblock copolymers. T_s was evaluated from a temperature variation of $I^{-1}(q_m)$ based on eq 39 for a given DP, and they used the theoretical $(N\chi)_s$ value for the ODT based on the original Leibler's theory[16] in order to determine χ_s. In the original Leibler's theory, however, the polydispersity and the asymmetry corrections are not involved.

Generally speaking, our result is in good agreement with the literature value in the lower temperature regime. In contrast to this, there is a considerably big difference in the higher temperature regime. The difference may be attributed to the difference of molecular weight, composition, architecture, and microstructure of the block copolymer. From the argument made above, the conventional asymmetry correction is a good approximation and therefore the difference between the result of Owens et al. and ours may be mainly ascribed to the above four factors inherent in the block copolymer. It is worth pointing out the asymmetry effect existing in their results. Although the conventional asymmetry correction is a good approximation, we found that this method likely underestimated the R_g values (see Table II). They have actually underestimated the R_g values compared to the values given from the molecular weight.

On the other hand, Hewel et al. have likely overestimated the $\chi_{S\text{-}B}$ values because the theory used is not corrected for the polydispersity and the asymmetry correction. However, the difference of the results on $\chi_{S\text{-}B}$ is not as big as that between the values evaluated by methods a and f. Since their method of determining χ is different from our method and the detailed sample characterization is not known, a further discussion is not warranted.

Finally it should be mentioned that poly(styrene-*block*-isoprene) (SI)/DOP[44] and mixtures of SI/homopolystyrene (HS)/DOP[45] tend to show $\chi_{eff} = \chi\phi_p^{0.7}$. However, this kind of ϕ_p dependence of χ_{eff} was not observed for the SBS/DOP systems with the polymer concentration ϕ_p in the range of $0.6 \lesssim \phi_p \leq 1.0$.

V. Concluding Remarks

In the present paper the scattering profiles of the triblock copolymers in the disordered state were analyzed by the RPA theory with the corrections for polydispersities in molecular weight and composition and asymmetry in the size and volume of the segment. Here the correction for the density fluctuation as reported by Fredrickson and Helfand,[19] Fredrickson and Leibler,[20] and Olvera de la Cruz[21] was not taken into account, since this theory might not be applied for the copolymers having DP smaller than 10^4, as stated in their reports, and this type of theory for the asymmetric and polydisperse A–B–A type triblock copolymer has not yet been developed. Recently Burger et al.[22] have proposed the theory on the ODT and the scattering function in the disordered state, which takes into account the density fluctuations along with the polydispersity correction for a pure diblock copolymer and its mixture with a homopolymer. A similar consideration on the A–B–A type triblock copolymer should be needed as a future work.

Acknowledgment. We are grateful to Dr. S. Yamauchi at the Mitsubishi Petrochemical Co., Ltd., for the characterization of the microstructure by ^{13}C NMR. This work is supported in part by a Grant-in-Aid for Scientific Research in Priority Areas "New Functionality Materials, Design, Preparation and Control" from the Ministry of Education, Science and Culture, Japan.

Appendix A

(i) $\langle S_{KJ}(q)\rangle_\nu$ for Asymmetric, Polydisperse A1–B–A2 Triblock Copolymers. We present here the analytical expressions of $\langle S_{KJ}(q)\rangle_\nu$ for asymmetric, polydisperse A1–B–A2 triblock copolymers obtained by the present approach using eqs 20–26 in the text.

$$\langle S_{AA}(q)\rangle_\nu = \frac{1}{r_{C,n}}\int_0^\infty\int_0^\infty\int_0^\infty [dN_{A1}\, dN_B\, dN_{A2}\, \varphi_{A1}(N_{A1}) \times \varphi_B(N_B)\, \varphi_{A2}(N_{A2})\, r_C^2\{f_{A1}^2 g_{A1}^{(2)}(q) + 2f_{A1}f_{A2}g_{A1}^{(1)}(q)\, g_{A2}^{(1)}(q)\exp(-x_B) + f_{A2}^2 g_{A2}^{(2)}(q)\}] = \frac{v_A^2}{r_{C,n}v_0^2}\int_0^\infty\int_0^\infty\int_0^\infty [dN_{A1}\, dN_B\, dN_{A2}\, \varphi_{A1}(N_{A1}) \times \varphi_B(N_B)\, \varphi_{A2}(N_{A2})\{N_{A1}^2 g_{A1}^{(2)}(q) + 2N_{A1}N_{A2}g_{A1}^{(1)}(q)\, g_{A2}^{(1)}(q)\exp(-x_B) + N_{A2}^2 g_{A2}^{(2)}(q)\}] \quad (A.1)$$

Similarly $\langle S_{BB}(q)\rangle_\nu$ and $\langle S_{AB}(q)\rangle_\nu$ are written as

$$\langle S_{BB}(q)\rangle_\nu = \frac{v_B^2}{r_{C,n}v_0^2}\int_0^\infty\int_0^\infty\int_0^\infty [dN_{A1}\, dN_B\, dN_{A2}\, \varphi_{A1}(N_{A1}) \times \varphi_B(N_B)\, \varphi_{A2}(N_{A2})\, N_B^2 g_B^{(2)}(q)] \quad (A.2)$$

$$\langle S_{AB}(q)\rangle_\nu = \frac{v_A v_B}{r_{C,n}v_0^2}\int_0^\infty\int_0^\infty\int_0^\infty [dN_{A1}\, dN_B\, dN_{A2}\, \varphi_{A1}(N_{A1}) \times \varphi_B(N_B)\, \varphi_{A2}(N_{A2})\{N_{A1}g_{A1}^{(1)}(q) + N_{A2}g_{A2}^{(1)}(q)\}N_B g_B^{(1)}(q)] \quad (A.3)$$

It is useful to calculate the following quantities:

$$\int_0^\infty\int_0^\infty\int_0^\infty dN_{A1}\, dN_B\, dN_{A2}\, \varphi_{A1}(N_{A1})\, \varphi_B(N_B) \times \varphi_{A2}(N_{A2})\, N_K^2 g_K^{(2)}(q) = \int_0^\infty dN_K\, \varphi_K(N_K)\, N_K^2 g_K^{(2)}(q) = \frac{2}{y_K^2}\int_0^\infty dN_K\, \varphi_K(N_K)\,[N_K y_K - 1 + \exp(-N_K y_K)] = \frac{2}{y_K^2}\left[N_{K,n}y_K - 1 + \left\{\frac{1}{N_{K,n}y_K(\lambda_K - 1) + 1}\right\}^{1/(\lambda_K - 1)}\right] = \frac{2N_{K,n}^2}{x_{K,n}^2}\left[x_{K,n} - 1 + \left\{\frac{1}{x_{K,n}(\lambda_K - 1) + 1}\right\}^{1/(\lambda_K - 1)}\right] = \left(\frac{v_0}{v_K}\right)^2 r_{C,n}^2 f_{K,n}^2 g_{K,n}^{(2)}(q) \quad (A.4)$$

and

$$\int_0^\infty\int_0^\infty\int_0^\infty dN_{A1}\,dN_B\,dN_{A2}\,\varphi_{A1}(N_{A1})\,\varphi_B(N_B)\,\varphi_{A2}(N_{A2})\times N_K g_K^{(1)}(q)\,N_L g_L^{(1)}(q) = \int_0^\infty dN_K\,\varphi_K(N_K)\,N_K g_K^{(1)}(q)\int_0^\infty dN_L \times \varphi_L(N_L)\,N_L g_L^{(1)}(q) = \frac{1}{y_K y_L}\int_0^\infty dN_K\,\varphi_K(N_K)\,[1-\exp(-N_K y_K)]\int_0^\infty dN_L\,\varphi_L(N_L)\,[1-\exp(-N_L y_L)] = \frac{1}{y_K}\left[1-\left\{\frac{1}{N_{K,n}y_K(\lambda_K-1)+1}\right\}^{1/(\lambda_K-1)}\right]\frac{1}{y_L}\left[1-\left\{\frac{1}{N_{L,n}y_L(\lambda_L-1)+1}\right\}^{1/(\lambda_L-1)}\right] = \frac{N_{K,n}}{x_{K,n}}\left[1-\left\{\frac{1}{x_{K,n}(\lambda_K-1)+1}\right\}^{1/(\lambda_K-1)}\right]\frac{N_{L,n}}{x_{L,n}}\left[1-\left\{\frac{1}{x_{L,n}(\lambda_L-1)+1}\right\}^{1/(\lambda_L-1)}\right] = \left(\frac{v_0}{v_K}\right)\left(\frac{v_0}{v_L}\right)r_{C,n}^2 f_{K,n}f_{L,n}g_{K,n}^{(1)}(q)\,g_{L,n}^{(1)}(q) \quad (A.5)$$

where

$$y_K = b_K^2 q^2/6 \quad (A.6)$$

$$x_{K,n} = N_{K,n}y_K = N_{K,n}b_K^2 q^2/6 \quad (A.7)$$

$$g_{K,n}^{(1)}(q) = \frac{1}{x_{K,n}}\left[1-\left\{\frac{1}{x_{K,n}(\lambda_K-1)+1}\right\}^{1/(\lambda_K-1)}\right] \quad (A.8)$$

$$g_{K,n}^{(2)}(q) = \frac{2}{x_{K,n}^2}\left[x_{K,n}-1+\left\{\frac{1}{x_{K,n}(\lambda_K-1)+1}\right\}^{1/(\lambda_K-1)}\right] \quad (A.9)$$

Using eqs A.4 and A.5, $\langle S_{KJ}(q)\rangle_\nu$'s are derived as

$$\langle S_{AA}(q)\rangle_\nu = r_{C,n}\left[f_{A1,n}^2 g_{A1,n}^{(2)}(q) + 2f_{A1,n}f_{A2,n}g_{A1,n}^{(1)}(q)\,g_{A2,n}^{(1)}(q)\left\{\frac{1}{x_{B,n}(\lambda_B-1)+1}\right\}^{1/(\lambda_B-1)} + f_{A2,n}^2 g_{A2,n}^{(2)}(q)\right] \quad (A.10)$$

$$\langle S_{BB}(q)\rangle_\nu = r_{C,n}f_{B,n}^2 g_{B,n}^{(2)}(q) \quad (A.11)$$

$$\langle S_{AB}(q)\rangle_\nu = r_{C,n}\{f_{A1,n}g_{A1,n}^{(1)}(q) + f_{A2,n}g_{A2,n}^{(1)}(q)\}f_{B,n}g_{B,n}^{(1)}(q) \quad (A.12)$$

(ii) $\langle S_{KJ}(q)\rangle_\nu$ for Asymmetric, Polydisperse A–B–A Triblock Copolymers. This is the special case of (i). The following expressions can be immediately obtained from eqs A.10–A.12.

$$\langle S_{AA}(q)\rangle_\nu = 2r_{C,n}f_{A,n}^2\left[g_{A,n}^{(2)}(q) + [g_{A,n}^{(1)}(q)]^2\left\{\frac{1}{x_{B,n}(\lambda_B-1)+1}\right\}^{1/(\lambda_B-1)}\right] \quad (A.13)$$

$$\langle S_{BB}(q)\rangle_\nu = r_{C,n}f_{B,n}^2 g_{B,n}^{(2)}(q) \quad (A.14)$$

$$\langle S_{AB}(q)\rangle_\nu = 2r_{C,n}f_{A,n}f_{B,n}g_{A,n}^{(1)}(q)\,g_{B,n}^{(1)}(q) \quad (A.15)$$

Appendix B

$\langle S_{KJ}(q)\rangle_\nu$ for Asymmetric, Polydisperse A–B Diblock Copolymers. We present here the analytical expression of $\langle S_{KJ}(q)\rangle_\nu$ for blends of asymmetric, polydisperse A–B diblock copolymers with polydisperse A and/or B homopolymers (the same systems as those we considered previously[31]) obtained by the present approach, using independence of the number distributions for the respective block chains; i.e., $\varphi(N_A,N_B) = \varphi_A(N_A)\,\varphi_B(N_B)$.

$$\langle S_{AA}(q)\rangle_\nu = \phi_C r_{C,n}f_{A,n}^2 g_{A,n}^{(2)}(q) + \phi_D r_{D,n}g_{D,n}^{(2)}(q) \quad (B.1)$$

$$\langle S_{BB}(q)\rangle_\nu = \phi_C r_{C,n}f_{B,n}^2 g_{B,n}^{(2)}(q) + \phi_E r_{E,n}g_{E,n}^{(2)}(q) \quad (B.2)$$

$$\langle S_{AB}(q)\rangle_\nu = \phi_C r_{C,n}f_{A,n}f_{B,n}g_{A,n}^{(1)}(q)\,g_{B,n}^{(1)}(q) \quad (B.3)$$

Here notations D and E designate A and B homopolymers, respectively, and ϕ_C, ϕ_D, and ϕ_E are volume fractions of A–B diblock copolymers and A and B homopolymers, respectively. $\phi_C + \phi_D + \phi_E = 1$.

Appendix C

$\langle S_{KJ}(q)\rangle_\nu$ for Asymmetric, Polydisperse A–B–A Triblock Copolymers (by the Previous Approach). We present here the analytical expressions of $\langle S_{KJ}(q)\rangle_\nu$ for asymmetric, polydisperse A–B–A triblock copolymers obtained by the previous approach[24] using eqs 30–32 instead of eqs 20–26 in the text. Here we show the results only for the case of $k_A = k_B = k$, $\lambda_A = \lambda_B = \lambda$.

$$\langle S_{AA}(q)\rangle_\nu = \frac{2r_{C,n}}{x_{A,n}^2}f_{A,n}^2(Q_{11}+Q_{12}-Q_{13}+Q_{14}-Q_{15}+Q_{16}) \quad (C.1)$$

with

$$Q_{11} = \frac{x_{A,n}}{f_{B,n}}F\left(1,k+2,2k+3;1-\frac{2f_{A,n}}{f_{B,n}}\right) \text{ for } f_{A,n}\le 0.25 = \frac{x_{A,n}}{2f_{A,n}}F\left(1,k+1,2k+3;1-\frac{f_{B,n}}{2f_{A,n}}\right) \text{ for } f_{A,n}>0.25 \quad (C.2)$$

$$Q_{12} = \frac{1}{f_{A,n}}\frac{1}{\lambda+1}(1+[\lambda-1]x_{A,n})^{-1/(\lambda-1)}\times F\left(1,k+1,2k+2;1-\frac{f_{B,n}}{2f_{A,n}}\{1+[\lambda-1]x_{A,n}\}\right) \text{ for } x_{A,n}\le\frac{1}{\lambda-1}\left(\frac{2f_{A,n}}{f_{B,n}}-1\right) = \frac{2}{f_{B,n}}\frac{1}{\lambda+1}(1+[\lambda-1]x_{A,n})^{-\lambda/(\lambda-1)}\times F\left(1,k+1,2k+2;1-\frac{2f_{A,n}}{f_{B,n}}\{1+[\lambda-1]x_{A,n}\}^{-1}\right) \text{ for } x_{A,n}>\frac{1}{\lambda-1}\left(\frac{2f_{A,n}}{f_{B,n}}-1\right) \quad (C.3)$$

$$Q_{13} = \frac{2}{f_{B,n}}\frac{1}{\lambda+1}F\left(1,k+1,2k+2;1-\frac{2f_{A,n}}{f_{B,n}}\right) \text{ for } f_{A,n}\le 0.25 = \frac{1}{f_{A,n}}\frac{1}{\lambda+1}F\left(1,k+1,2k+2;1-\frac{f_{B,n}}{2f_{A,n}}\right) \text{ for } f_{A,n}>0.25 \quad (C.4)$$

$$Q_{14} = \frac{1}{f_{B,n}}\frac{1}{\lambda+1}\{1+[\lambda-1]x_{B,n}\}^{-1/(\lambda-1)} \times F\left(1,k+1,2k+2;1-\frac{2f_{A,n}}{f_{B,n}}\{1+[\lambda-1]x_{B,n}\}\right) \quad \text{for } x_{B,n} \le \frac{1}{\lambda-1}\left(\frac{f_{B,n}}{2f_{A,n}}-1\right)$$

$$= \frac{1}{2f_{A,n}}\frac{1}{\lambda+1}\{1+[\lambda-1]x_{B,n}\}^{-\lambda/(\lambda-1)} \times F\left(1,k+1,2k+2;1-\frac{f_{B,n}}{2f_{A,n}}\{1+[\lambda-1]x_{B,n}\}^{-1}\right) \quad \text{for } x_{B,n} > \frac{1}{\lambda-1}\left(\frac{f_{B,n}}{2f_{A,n}}-1\right) \tag{C.5}$$

$$Q_{15} = \frac{2}{f_{B,n}}\frac{1}{\lambda+1}\{1+[\lambda-1]x_{A,n}\}^{-\lambda/(\lambda-1)} \times \{1+[\lambda-1]x_{B,n}\}^{-1/(\lambda-1)}F\left(1,k+1,2k+2;1-\frac{2f_{A,n}}{f_{B,n}}\frac{1+[\lambda-1]x_{B,n}}{1+[\lambda-1]x_{A,n}}\right) \quad \text{for } \frac{1}{2f_{A,n}}(1+[\lambda-1]x_{A,n}) \ge \frac{1}{f_{B,n}}(1+[\lambda-1]x_{B,n})$$

$$= \frac{1}{f_{A,n}}\frac{1}{\lambda+1}\{1+[\lambda-1]x_{A,n}\}^{-1/(\lambda-1)} \times \{1+[\lambda-1]x_{B,n}\}^{-\lambda/(\lambda-1)}F\left(1,k+1,2k+2;1-\frac{f_{B,n}}{2f_{A,n}}\frac{1+[\lambda-1]x_{A,n}}{1+[\lambda-1]x_{B,n}}\right) \quad \text{for } \frac{1}{2f_{A,n}}(1+[\lambda-1]x_{A,n}) < \frac{1}{f_{B,n}}(1+[\lambda-1]x_{B,n}) \tag{C.6}$$

$$Q_{16} = \frac{1}{f_{B,n}}\frac{1}{\lambda+1}\{1+2[\lambda-1]x_{A,n}\}^{-\lambda/(\lambda-1)} \times \{1+[\lambda-1]x_{B,n}\}^{-1/(\lambda-1)}F\left(1,k+1,2k+2;1-\frac{2f_{A,n}}{f_{B,n}}\frac{1+[\lambda-1]x_{B,n}}{1+2[\lambda-1]x_{A,n}}\right) \quad \text{for } \frac{1}{2f_{A,n}}(1+2[\lambda-1]x_{A,n}) \ge \frac{1}{f_{B,n}}(1+[\lambda-1]x_{B,n})$$

$$= \frac{1}{2f_{A,n}}\frac{1}{\lambda+1}\{1+2[\lambda-1]x_{A,n}\}^{-1/(\lambda-1)} \times \{1+[\lambda-1]x_{B,n}\}^{-\lambda/(\lambda-1)}F\left(1,k+1,2k+2;1-\frac{f_{B,n}}{2f_{A,n}}\frac{1+2[\lambda-1]x_{A,n}}{1+[\lambda-1]x_{B,n}}\right) \quad \text{for } \frac{1}{2f_{A,n}}(1+2[\lambda-1]x_{A,n}) < \frac{1}{f_{B,n}}(1+[\lambda-1]x_{B,n}) \tag{C.7}$$

where $F(\alpha,\beta,\gamma;z)$ is the Gauss hypergeometric function.

$$\langle S_{BB}(q)\rangle_\nu = \frac{2r_{C,n}}{x_{B,n}}f_{B,n}^{\,2}(Q_{21}+Q_{22}-Q_{23}) \tag{C.8}$$

with

$$Q_{21} = \frac{x_{B,n}}{2f_{B,n}}F\left(1,k+1,2k+3;1-\frac{2f_{A,n}}{f_{B,n}}\right) \quad \text{for } f_{A,n} \le 0.25$$

$$= \frac{x_{B,n}}{4f_{A,n}}F\left(1,k+2,2k+3,1-\frac{f_{B,n}}{2f_{A,n}}\right) \quad \text{for } f_{A,n} > 0.25 \tag{C.9}$$

$$Q_{22} = Q_{14} \tag{C.10}$$

$$Q_{23} = Q_{13}/2 \tag{C.11}$$

and

$$\langle S_{AB}(q)\rangle_\nu = \frac{2r_{C,n}}{x_{A,n}x_{B,n}}f_{A,n}f_{B,n}(Q_{31}-Q_{32}-Q_{33}+Q_{34}) \tag{C.12}$$

with

$$Q_{31} = Q_{13}/2 \tag{C.13}$$

$$Q_{32} = Q_{12}/2 \tag{C.14}$$

$$Q_{33} = Q_{14} \tag{C.15}$$

$$Q_{34} = Q_{15}/2 \tag{C.16}$$

References and Notes

(1) Roe, R.-J.; Fishkis, M.; Chang, C. J. *Macromolecules* **1981**, *14*, 1091.
(2) Hashimoto, T. In *Thermoplastic Elastomers*; Legge, N. R., Holden, G., Schroeder, H. E., Eds.; Hanser: Vienna, 1987; Chapter 12, Section 3, p 349.
(3) Hashimoto, T.; Shibayama, M.; Kawai, H. *Macromolecules* **1983**, *16*, 1093.
(4) Mori, K.; Hasegawa, H.; Hashimoto, T. *Polym. J. (Tokyo)* **1985**, *17*, 799.
(5) Hashimoto, T.; Ijichi, Y.; Fetters, L. J. *J. Chem. Phys.* **1988**, *89*, 2463. Ijichi, Y.; Hashimoto, T.; Fetters, L. J. *Macromolecules* **1989**, *22*, 2817.
(6) Han, C. D.; Baek, D. M.; Sakurai, S.; Hashimoto, T. *Polym. J. (Tokyo)* **1989**, *21*, 841.
(7) Owens, J. N.; Gancarz, I. S.; Koberstein, J. T.; Russell, T. P. *Macromolecules* **1989**, *22*, 3380.
(8) Hewel, M.; Ruland, W. *Makromol. Chem., Macromol. Symp.* **1986**, *4*, 197.
(9) de Gennes, P.-G. *Scaling Concepts in Polymer Physics*; Cornell University Press: Ithaca, NY, 1979.
(10) Bates, F. S.; Hartney, M. A. *Macromolecules* **1985**, *18*, 2478; **1986**, *19*, 2892.
(11) Bates, F. S.; Rosedale, J. H.; Fredrickson, G. H. *J. Chem. Phys.* **1990**, *92*, 6255.
(12) Almdal, K.; Rosedale, J. H.; Bates, F. S.; Wignall, G. D.; Fredrickson, G. H. *Phys. Rev. Lett.* **1990**, *65*, 1112.
(13) Benoit, H.; Wu, W.; Benmouna, M.; Mozer, B.; Bauer, B.; Lapp, A. *Macromolecules* **1985**, *18*, 986.
(14) Han, C. D.; Kim, J.; Kim, J. K. *Macromolecules* **1989**, *22*, 383.
(15) Rosedale, J. H.; Bates, F. S. *Macromolecules* **1990**, *23*, 2329.
(16) Leibler, L. *Macromolecules* **1980**, *13*, 1602.
(17) Olvera de la Cruz, M.; Sanchez, I. C. *Macromolecules* **1986**, *19*, 2501.
(18) Benoit, H.; Hadziioannou, G. *Macromolecules* **1988**, *21*, 1449.
(19) Fredrickson, G. H.; Helfand, E. *J. Chem. Phys.* **1987**, *87*, 697.
(20) Fredrickson, G. H.; Leibler, L. *Macromolecules* **1989**, *22*, 1238.
(21) Olvera de la Cruz, M. *J. Chem. Phys.* **1989**, *90*, 1995.
(22) Burger, C.; Ruland, W.; Semenov, A. N. *Macromolecules* **1990**, *23*, 3339.
(23) Mori, K.; Tanaka, H.; Hashimoto, T. *Macromolecules* **1987**, *20*, 381.
(24) Mori, K.; Tanaka, H.; Hasegawa, H.; Hashimoto, T. *Polymer* **1989**, *30*, 1389.
(25) Hashimoto, T.; Mori, K. *Macromolecules* **1990**, *23*, 5347.
(26) Inoue, T.; Hashimoto, T., in preparation.
(27) Leibler, L.; Benoit, H. *Polymer* **1981**, *22*, 195.
(28) Benmouna, M.; Benoit, H. *J. Polym. Sci., Polym. Phys. Ed.* **1983**, *21*, 1227.
(29) Hong, K. M.; Noolandi, J. *Polym. Commun.* **1984**, *25*, 265.
(30) Ijichi, Y.; Hashimoto, T. *Polym. Commun.* **1988**, *29*, 135.
(31) Tanaka, H.; Sakurai, S.; Hashimoto, T.; Whitmore, M. D. *Polymer* **1992**, *33*, 1006.
(32) Brazovskii, S. A. *Sov. Phys. JETP* **1975**, *41*, 85.
(33) Onuki, A.; Hashimoto, T. *Macromolecules* **1989**, *22*, 879.
(34) Hashimoto, T.; Suehiro, S.; Shibayama, M.; Saijo, K.; Kawai, H. *Polym. J. (Tokyo)* **1981**, *13*, 501.
(35) Fujimura, M.; Hashimoto, T.; Kawai, H. *Mem. Fac. Eng., Kyoto Univ.* **1981**, *43* (2), 224.
(36) Hendricks, R. W. *J. Appl. Cryst.* **1972**, *5*, 315.
(37) Note for the thermal expansivity of the unperturbed chain dimension. For the multiblock copolymers the thermal expansivity κ may be given by $\kappa = \sum_K[\kappa_K\langle R_K^2(T)\rangle_0/\langle R^2(T)\rangle_0]$ where $\langle R_K^2(T)\rangle_0$ and κ_K denote a mean-square end-to-end distance of the K block chains at a given T and its temperature coefficient, respectively. With the literature values of κ, -1.1×10^{-3} [K^{-1}] for polystyrene[39] and -0.10×10^{-3} [K^{-1}] for 1,4-polybutadiene,[46] we obtained $\kappa = -0.3 \times 10^{-3}$ [K^{-1}] for the particular SBS samples used in this work.
(38) Since the theoretical SAXS profile is sensitively influenced by the polydispersity, accuracy of the value M_w/M_n is necessary. The value obtained by GPC, however, varies within 0.15

depending on the apparatus used, which is noted in Table I. It is inadvisable to use its average value. Therefore, we let M_w/M_n be a floating parameter in the fitting analyses. The best fits gave the values of M_w/M_n as 1.13 and 1.16 for TR-1102 and D-1102, respectively.

(39) Mays, J. W.; Hadjichristidis, N.; Fetters, L. J. *Macromolecules* **1985**, *18*, 2231.
(40) Fetters, L. J., private communication.
(41) Mays, J.; Hadjichristidis, N.; Fetters, L. J. *Macromolecules* **1984**, *17*, 2723.
(42) Sakurai, S.; Hasegawa, H.; Hashimoto, T.; Han, C. C. *Polym. Commun.* **1990**, *31*, 99.
(43) Sakurai, S.; Izumitani, T.; Hasegawa, H.; Hashimoto, T.; Han, C. C. *Macromolecules* **1991**, *24*, 4844.
(44) Hashimoto, T.; Mori, K., in preparation.
(45) Tanaka, H.; Hashimoto, T. *Macromolecules* **1991**, *24*, 5398.
(46) Mays, J. W.; Hadjichristidis, N.; Graessley, W. W.; Fetters, L. J. *J. Polym. Sci., Part B: Polym. Phys. Ed.* **1986**, *24*, 2553.

Registry No. DOP, 117-81-7.